ANALYSIS OF LOCAL DELAMINATION IN COMPOSITE LAMINATES WITH CROSS PLY MATRIX CRACKS

M. Kashtalyan*, J. Zhang+, C. Soutis*

The total strain energy release rate G associated with delaminations that initiate and grow uniformly from the cross ply matrix crack tip in the $-\theta/90$ interfaces of symmetric composite laminates is calculated using the potential energy approach and a two-dimensional (2-D) finite element (FE) analysis. On examining of carbon fibre-epoxy resin laminates, it is found that the shear mode (Mode II) dominates the growth of delamination. The total strain energy release rate increases with increasing delamination length, but eventually approaches a constant asymptotic value, which is close to the result calculated from the analytical model. Analytical and numerical calculations show that G for local delamination decreases notably with increasing matrix cracking.

INTRODUCTION

Matrix cracking in the transverse (90°) plies is the first damage mode observed in a $[\pm\theta_m/90_n]_s$ balanced symmetric laminate subjected to static or fatigue tensile loading. It multiplies with increasing applied load, and subsequently, either edge delamination will form between the interface or local delamination will initiate from the transverse ply crack tips due to high local stresses at the crack tip. A review of micromechanical models that have been developed over the years for the prediction of multiple matrix cracking in uni- and biaxially loaded cross-ply laminates was made by McCartney (1). A number of researchers have shown that the strain energy release rate G associated with local delamination can be compared with an appropriate value of interlaminar fracture toughness, obtained experimentally following Martin and Murri (2), to estimate the initiation and propagation of delamination. A closed-form equation for G, which for certain lay-ups can successfully predict the delamination onset strain, was derived by O'Brien (3, 4). However, he neglected the effect of matrix ply cracking which becomes important for thick 90-ply laminates where local delaminations usually develop. More recently, Zhang and Soutis (5) modelled the matrix crack tip delamination and its effect on the stiffness properties of

* Department of Aeronautics, Imperial College, London SW7 2BY, UK
+ Department of Engineering Mechanics, Chongqing University, 400044 Chongqing, China

carbon fibre-epoxy laminates. A 2-D shear lag approach was proposed to obtain the microstress field in the damaged laminate. These resulting microstresses were used in the *in situ* damage effective functions (IDEFs) which were derived explicitly in terms of matrix crack density and relative local delamination area. Then, expressions for the strain energy release rates for matrix cracking and local delamination were derived, taking into account the interaction effect between the two damage modes. In the present study theoretical modelling and a 2-D plain strain FE analysis are used to estimate the total strain energy release rate G associated with local delamination for different matrix crack densities. On the basis of the theoretically predicted energy release rate and Griffith's energy criterion the delamination onset strain is determined.

STRAIN ENERGY RELEASE RATE

Suppose transverse ply cracks exist in the 90° plies with a uniform crack spacing of $2s$, and local delaminations initiate and grow from both tips of each crack, spanning the width of the specimen. In order to examine the effect of these damage modes on the laminate loading capacity a representative three-layer segment containing a single transverse ply crack and two strip-shaped delaminations is considered (Figure 1). This element can be segregated into a locally delaminated region $0 \le y \le \ell_d$ and a laminated region $\ell_d \le y \le s$.

The potential energy method developed by Zhang et al (6) is used to derive expressions for the energy release rates associated with the local delamination, matrix cracking, and their interaction. The potential energy of the 'equivalent' damaged laminate element with a finite gauge length of 2ℓ and width of w is

$$PE = \frac{w2\ell}{2}\sum_{k=1}^{n}(z_k - z_{k-1})\{\varepsilon\}^{\mathrm{T}}[\overline{Q}]_k\{\varepsilon\} - \{N\}^{\mathrm{T}}\{\varepsilon\}2\ell w, \quad \{N\} = \sum_{k=1}^{n}\int_{z_{k-1}}^{z_k}\{\sigma\}_k\,dz \quad (1)$$

where $\{\sigma\}_k$ the macrostress in the k-th ply group, $\{\varepsilon\}$ is the strain vector and $[\overline{Q}]_k$ is the damaged lamina reduced stiffness matrix. The energy release rate associated with a particular damage mode is equal to the first partial derivative of the potential energy with respect to the crack surface area of the respective damage; the applied laminate loads, $\{N\}$, are fixed and the other damage modes remain unchanged. So, the strain energy release rate due to local delamination is, for instance,

$$G^{ld} = -\left[\frac{\partial PE}{\partial A^{ld}}\right]_{\{N\},A^{mc}}, \quad A^{ld} = 2\ell w D^{ld}, \quad A^{mc} = 2\ell w D^{mc} \quad (2)$$

Knowing the in-plane stiffness matrix of the cracked lamina for a given relative matrix crack density, $D^{mc} = h_2 / s$, and relative local delamination area, $D^{ld} = \ell_d / s$, the energy release rate can be directly evaluated by differentiating the reduced stiffness matrix with respect to the corresponding damage variable, i.e.

$$G^{ld}(\varepsilon, D^{mc}, D^{ld}) = -\frac{h_2}{2}\{\varepsilon\}^{\mathrm{T}}\frac{\partial[\overline{Q}]_2}{\partial D^{ld}}\{\varepsilon\}, \quad (3)$$

The effect of interaction between the matrix cracking and local delamination is explicitly included in the expression of the *in situ* damage effective functions (IDEFs) Λ_{ij} which are used to obtain the reduced stiffness matrix, $[\overline{Q}]$. The modified stiffness matrix of a cracked lamina is given by:

$$[\overline{Q}]=\begin{bmatrix} Q_{11}^0 & Q_{12}^0 & 0 \\ Q_{12}^0 & Q_{22}^0 & 0 \\ 0 & 0 & Q_{66}^0 \end{bmatrix}-\begin{bmatrix} (Q_{12}^0)^2(Q_{22}^0)^{-1}\Lambda_{22} & Q_{12}^0\Lambda_{22} & 0 \\ Q_{12}^0\Lambda_{22} & Q_{22}^0\Lambda_{22} & 0 \\ 0 & 0 & Q_{66}^0\Lambda_{66} \end{bmatrix} \tag{4}$$

where $[Q^0]$ is the in-plane stiffness matrix of the 90° (ply 2) uncracked lamina. Functions Λ_{22} and Λ_{66} were calculated on the basis of a 2-D shear-lag analysis assuming that the out-of-plane shear stresses varied linearly across the thickness of the constraining layer (ply 1) and are given by

$$\Lambda_{22}=1-\frac{\Phi_1(1-D^{ld})+\Phi_2 D^{mc}\tanh[\lambda_1(1-D^{ld})/D^{mc}]}{\Phi_1(1+\zeta_1 D^{ld})+\Phi_3 D^{mc}\tanh[\lambda_1(1-D^{ld})/D^{mc}]}$$
$$\Lambda_{66}=1-\frac{\Gamma_1(1-D^{ld})+\Gamma_2 D^{mc}\tanh[\lambda_2(1-D^{ld})/D^{mc}]}{\Gamma_1(1+\zeta_2 D^{ld})+\Gamma_3 D^{mc}\tanh[\lambda_2(1-D^{ld})/D^{mc}]} \tag{5}$$

where the parameters $\Phi_i, \Gamma_i, \zeta_i, \lambda_i$ are laminate constants. When delamination is ignored, the above expressions reduce to the corresponding relations for pure matrix cracking derived by Zhang et al (7, 8).

The present analytical model and O'Brien's simple equation for G obtained in reference (4) are assessed by a 2-D FE analysis of the three-layer sandwich element used above. The FE package ABAQUS is employed to obtain the interlaminar stresses and the strain energy release rate associated with a local delamination starting from the transverse ply cracks. The energy release rate, G^{ld}, in the FE model is evaluated using the virtual crack closure technique (VCCT) suggested by Rybicki and Kanninen (9).

NUMERICAL RESULTS FOR CFRP LAMINATES

The present analytical model is compared with the 2-D FE solution and O'Brien's simple model (4). As an example, the energy release rate associated with local delamination is calculated for the T300/934 $[\pm 25/90_4]_s$ laminate. The stiffness properties of the T300/934 graphite/epoxy system are taken equal to: $E_{11}=144.8\text{GPa}$, $E_{22}=E_{33}=11.38\,\text{GPa}$, $G_{12}=G_{13}=6.48\,\text{GPa}$, $G_{23}=3.45\,\text{GPa}$, $\nu_{12}=\nu_{23}=0.3$ and $t=0.132\,\text{mm}$. It is found that the energy release rate, equation (3), varies linearly with the square of the applied axial stress or strain. This implies that the energy release rate can be normalised by the applied axial strain, ε_y, to study the effect of damage separately. The comparisons between the present theory, O'Brien's model and the 2-D FE analysis are shown in Figures 2, 3. The energy release rate normalised by the applied strain is plotted against the relative local

delamination area, D^{ld}, for two matrix crack densities $C_d = (2s)^{-1} = 0.947\text{cm}^{-1} = 80t$ and $C_d = 4.38\text{cm}^{-1}$. The FE solution shows that the normalised energy release rate increases with increasing delamination length, approaching a constant asymptotic value. This value is close to the prediction given by the present analytical model. It can be seen that the strain energy release rate for delamination is reduced with increasing matrix crack density. The present analytical model agrees well with the FE solution in the steady-state growth of delamination. The predictions based on O'Brien's simple equation are far away from the FE results. However, further development of the model is required in the transient delamination range (small delamination lenghts).

In order to evaluate the critical load for local delamination initiation, the Griffith's energy release rate criterion is expressed as

$$G^{ld}(\bar{\varepsilon}, D^{mc}, D^{ld}) = G_c^{ld} \tag{6}$$

where G_c^{ld} is the interlaminar fracture toughness of the composite material. For the examined T300/934 carbon-epoxy system, G_c^{ld} is taken as $310\,\text{J/m}^2$. To obtain the delamination onset strain from the above equation, the matrix crack density at which local delamination initiates is required; this particular matrix crack density value varies with lay-up. For the $[\pm 25/90_4]_s$ laminates tested by Crossman and Wang (10) it can be inferred from the delamination onset strain and transverse ply crack density/strain data given in reference (10). Using equation (3) for energy release rate associated with local delamination, the local delamination onset strain is obtained by solving equation (6). Figure 4 gives the delamination onset strain as a function of the number of 90° plies in the $[\pm 25/90_4]_s$ laminates. The dash line is the predicted local delamination onset strain. In the experiments, the damage undergoes a transition from edge delamination ($n \le 4$) to local delamination ($n \ge 4$). The prediction is in good agreement with experimental data for $n \ge 4$. For $n \le 4$, the edge delamination is the dominant damage mode and has been analysed in (5).

CONCLUSIONS

Balanced symmetric $[\pm\theta_m / 90_n]_s$ composite laminates containing ply cracks and loaded in tension were studied using a new theoretical model and a 2-D FE analysis. Matrix cracks were assumed to be present in the 90° plies with local delaminations growing uniformly from the matrix crack tip at the $-\theta/90$ interface. The total strain energy release rate for delamination was evaluated. The FE result was in good agreement with theoretical predictions for large delaminations and was substantially affected by the matrix crack density. Further work is required in order to examine damage configurations where delaminations do not grow uniformly across the laminate width. A 3-D FE analysis is needed to study the contribution of mode III on the growth of local delamination.

REFERENCES

(1) McCartney, L.N., J de Physique III, Vol.3, No.11, 1993, pp.1637-1646.
(2) Martin, R.H., and Murri, G.B. ASTM STP 1059, 1990, pp. 251-270.

(3) O'Brien, K.T. ASTM STP 775, pp.140-167.
(4) O'Brien, K.T. ASTM STP 876, 1985, pp.282-297.
(5) Zhang, J., and Soutis, C. LUED TR.92, 1992.
(6) Zhang, J., Fan, J. and Soutis, C. Adv. Composite Letters, Vol.1, 1992, pp.12-15.
(7) Zhang, J., Fan, J. and Soutis, C. Composites, Vol.23, No.5, 1992, pp.299-304.
(8) Zhang, J., Fan, J. and Soutis, C. Composites, Vol.23, No.5, 1992, pp.299-304.
(9) Rybicki, E.F., and Kanninen, M.F. Eng. Fract. Mech., Vol.9, 1977, pp.931-938.
(10) Crossman, F.W., and Wang, A.S. ASTM STP 775, 1982, pp. 118-139.

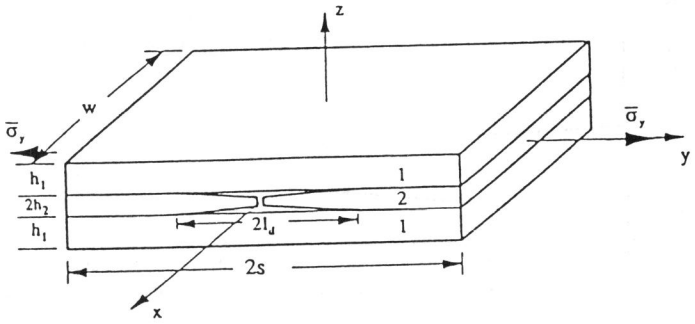

Figure 1 Representative segment with local delamination growing from a matrix crack

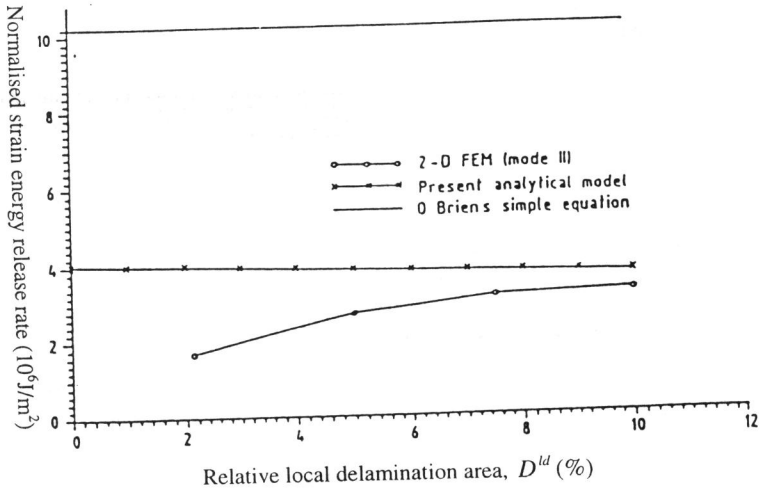

Figure 2 Change in G/ε_y due to uniform delamination growth for $C_d = 0.947\text{cm}^{-1}$

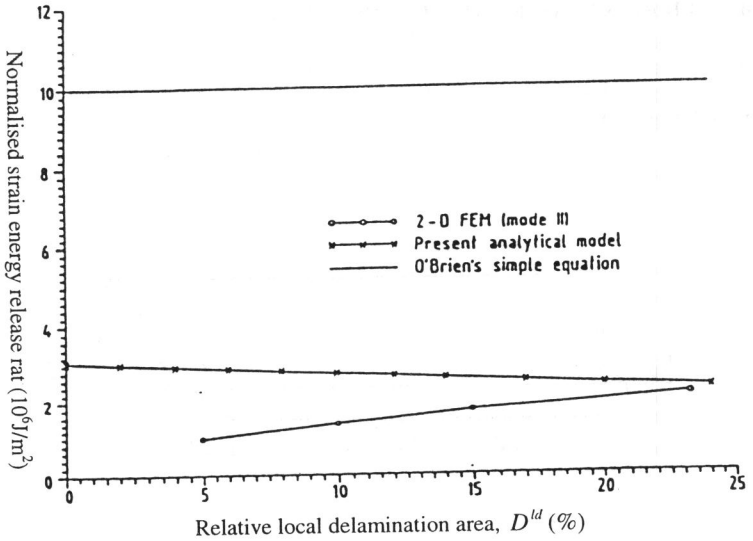

Figure 3 Change in G/ε_y due to uniform delamination growth for $C_d = 4.38\text{cm}^{-1}$

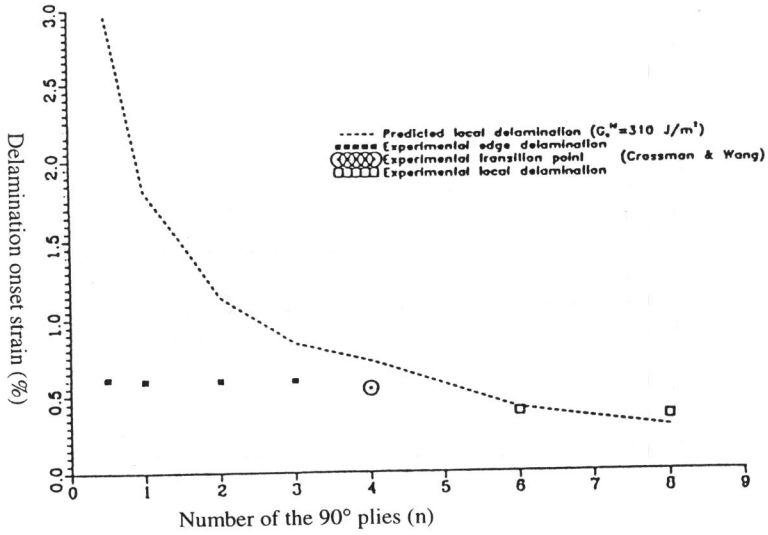

Figure 4 Delamination onset strain